Published in final edited form as:
Mol Cancer Ther. 2008 April ; 7(4): 923–934. doi:10.1158/1535-7163.MCT-07-0540.

SUMOylation of HMGA2: selective destabilization of promyelocytic leukemia protein via proteasome

Xuefei Cao[1], **Carlos Clavijo**[1], **Xu Li**[1,2], **H. Helen Lin**[2], **Yuan Chen**[3], **Hsiu-Ming Shih**[4], and **David K. Ann**[1,2]

[1] Department of Pharmacology and Pharmaceutical Sciences, University of Southern California, Los Angeles, California

[2] Department of Molecular and Clinical Pharmacology, City of Hope, Duarte National Medical Center, Duarte, California

[3] Department of Immunology, City of Hope, Duarte National Medical Center, Duarte, California

[4] Institute of Biomedical Sciences, Academia Sinica, Taipei, Taiwan, Republic of China

Abstract

The HMGA2 architectural protein functions in a variety of cellular processes, such as cell growth, transcription regulation, neoplastic transformation, and progression. Up-regulation of HMGA2 protein is observed in many tumors and is associated with advanced cancers with poor prognoses. Although the expression and biochemical properties of HMGA2 protein are regulated by microRNA and phosphorylation, it is unknown whether HMGA2 activity can also be regulated by SUMOylation, and that is what is investigated in this report. We identified HMGA2 as a SUMOylation target and showed that the expression of wild-type HMGA2, but not SUMOylation-defective HMGA2(2K/R), selectively lowered the steady-state level of PML protein. Consequently, the HMGA2-elicited PML down-regulation rendered a reduction in the average number of PML nuclear bodies per cell and the volume of PML assembled per PML nuclear body. Using small interfering RNA to suppress endogenous ubiquitin expression and proteasome inhibitor to repress ubiquitin-mediated protein degradation, we showed that HMGA2 confers PML down-regulation through ubiquitin-proteasome–dependent protein degradation. Importantly, arsenic trioxide treatment stimulated HMGA2 SUMOylation, leading to the formation of HMGA2 nuclear foci surrounding PML nuclear bodies and the stimulation of PML degradation. Collectively, our results unveil a previously unrecognized effect by HMGA2 on the modulation of PML protein level, providing a novel mechanism underlying HMGA2 function and underscoring the molecular basis for oncogenic progression by HMGA2.

Introduction

Members of the high mobility group A (HMGA1a, HMGA1b, and HMGA2) family of architectural transcription factors are distinguished by three reiterated “AT hooks” of 10 to 12 residues in each DNA binding motif, and they are critical for a variety of cellular processes, including gene transcription, induction of neoplastic transformation, and promotion of metastatic progression (1,2). The expression level of HMGA2 is maximal during early stages of fetal development but is low in terminally differentiated cells (1). A strong correlation has been established between HMGA2 protein expression and the relevant oncogenic phenotypes.

Requests for reprints: David K. Ann, Department of Clinical and Molecular Pharmacology, City of Hope, 1500 East Duarte Road, Duarte, CA 91010. Phone: 626-359-8111, ext. 64967; Fax: 626-471-7204. dann@coh.org.
Note: X. Li and C. Clavijo contributed equally to this work.

First, HMGA2 expression is implicated in malignant phenotypes of mesenchymal as well as epithelial origin (3–5). Second, the evidence for its direct role in tumorigenesis came from transfection of an antisense DNA against HMGA2 in the normal thyroid cells that prevented the neoplastic transformation induced by myeloproliferative sarcoma virus and Kristen murine sarcoma virus (6). In addition, the transgenic mice overexpressing HMGA2 developed pituitary adenomas (7). Third, the expression of HMGA2 in oral squamous cell carcinoma is associated with increased disease recurrence and metastasis, along with a reduced survival rate manifested by a facilitated epithelial-mesenchymal transition (8). Moreover, HMGA2 expression is associated with the poor prognosis and metastasis in patients with breast cancer (9).

Covalent attachment of ubiquitin and small ubiquitin-like modifier (SUMO) to proteins plays a major role in regulating cellular functions (10–12). Both modifications depend on similar, but distinct, enzyme cascades. Briefly, ubiquitin and SUMO are activated in an ATP-dependent manner by individual E1-activating enzymes, transferred to the respective E2-conjugating enzymes and subsequently attached to the Lys acceptor sites of target proteins by distinct E3 ligases. Whereas ubiquitination generally promotes protein degradation, SUMOylation largely serves to regulate diverse cellular processes, including nuclear transport, genome integrity, signal transduction, and transcriptional regulation (10–12). The list of known SUMO targets has grown substantially in recent years, and over half of the presently identified SUMO targets are transcription factors or coregulators, attenuating transcriptional activation (10–12). Additionally, SUMOylation has been shown to affect the dynamic interaction between transcription regulator(s) and promyelocytic leukemia (PML) protein (13,14). PML is essential for the formation of a nuclear matrix–associated multiprotein complex, namely the PML nuclear body (15). PML and PML nuclear bodies have been implicated in governing a variety of cellular processes, including transcriptional regulation, tumor suppression, cellular senescence, apoptosis, and immune responses (16–18).

In searching for HMGA2-interacting proteins and possible molecular mechanisms by which HMGA2 functions as an oncogene, we identified SUMO E2 conjugase Ubc9 and SUMO-1 as such partners, suggesting HMGA2 as a potential target for SUMO conjugation. In this study, we show that the expression of HMGA2 resulted in the SUMOylation-dependent down-regulation of PML, but not RanGAP-1 and GR, protein level and a concordant reduction in the average size and number of PML nuclear bodies. Moreover, the observed HMGA2-dependent PML down-regulation was partially reversed by small interfering RNA (siRNA) against ubiquitin or proteasome inhibitor, suggesting the involvement of ubiquitin-proteasome–dependent protein degradation. Together, these observations led us to propose a novel function for HMGA2, which uses a SUMO-dependent mechanism(s) to selectively promote the degradation of PML protein, perturbing the dynamic network and multiple functions associated with PML.

Materials and Methods

Cell Culture

The rat parotid epithelial cell line Pa-4, also known as parotid C5 cells, was plated on Primaria culture dishes (Falcon) in DMEM/Ham's F-12 (1:1) medium supplemented with 2.5% FCS, insulin (5 μg/mL), transferrin (5 μg/mL), epidermal growth factor (25 ng/mL), hydro-cortisone (1.1 μmol/L), glutamine (5 mmol/L), and kanamycin monosulfate (60 μg/mL) and maintained in a humidified atmosphere of 5% CO_2, 95% air at 35°C (19). The HeLa/HMGA2 cells were established by stably transfecting HeLa cells with pcDNA3.1-HA-HMGA2, followed by a selection with G418 (1000 μg/mL). The HeLa/HMGA2 and Pa-4/HMGA2 cells were maintained in medium supplemented with G418 (600 μg/mL). HeLa, HeLa/HMGA2, and COS-1 cells were cultured in a humidified atmosphere of 5% CO_2, 95% air at 37°C.

Construct Engineering and siRNA

HMGA2 mutant carrying K66R and K67R mutations was generated using HA-HMGA2/pcDNA3.1 that we previously described (20) as a template in conjunction with GeneEditor *in vitro* Site-Directed Mutagenesis System (Promega) with designed mutagenesis primer pairs. To generate pCMV-Tag2A-SUMO-HMGA2 fusion constructs, SUMO-1 (amino acid 1–96) was amplified by PCR and the PCR-amplified SUMO-1 (1–96) fragment was inserted between *Bam*HI and *Hin*dIII in the multiple cloning sites of pCMV-Tag2A. Subsequently, the HMGA2 or HMGA2 (2K/R) coding region was cloned downstream of the resulting pCMV-Tag2A-SUMO-1 between *Hin*dIII and *Xho*I. The sequences of derived constructs were verified by DNA sequencing. The ubiquitin siRNA (h) was purchased from Santa Cruz Biotechnology, Inc. The sense and antisense oligonucleotides were individually dissolved in RNase-free water at 100 μmol/L and subsequently annealed by heating at 90°C for 1 min, and incubating at 37° C for 1 h at a concentration of 20 μmol/L. Transfection of siRNA was done with Lipofectamine 2000 (Invitrogen) according to the manufacturer's instruction.

Rat deSUMOylase ΔAxam was cloned by reverse transcription-PCR using total RNA extracted from rat parotid Pa-4 cells. Oligo-dT primer was used in the reverse transcription reaction, whereas the deSUMOylase-specific primer pairs used in the PCR reactions were designed according to rat ΔAxam sequence in Genbank (21). The resulting PCR products were first cloned into TA-cloning vector pCR2.1-TOPO (Invitrogen) and subsequently into the FLAG-tagged expression vector pCMV-Tag3B (Strata-gene). Expression of the resulting constructs was confirmed by transient transfection into Pa-4 cells followed by Western analysis using anti-FLAG antibody. As compared with the mock-transfected control, a unique and intense protein band at 60 kDa, corresponding to ΔAxam, was observed in total cell lysates prepared from transfected cell lysates (data not shown).

Cell Lysis and Western Analyses

Cells were washed twice in ice-cold 1× PBS and lysed in SDS sample loading buffer. Equal amounts of proteins from total cell extracts were fractionated by electrophoresis on SDS-PAGE and were electroblotted onto an Immobilon-P membrane (Millipore). The membrane was blocked with 5% nonfat milk and 0.1% Tween 20 in TBS for 1 h at room temperature and incubated with the respective primary antibodies, including anti-GR (Santa Cruz Biotechnology), anti-HA (Covance), anti-PML (Santa Cruz Biotechnology), anti-GMP (Zymed Laboratories, Inc.), anti-actin (Chemicon), anti-His (Santa Cruz Biotechnology), and anti-GFP (Santa Cruz Biotechnology). Horseradish peroxidase–conjugated goat–anti-rabbit IgG (Santa Cruz Biotechnology) or goat–anti-mouse IgG (Santa Cruz Biotechnology) was used to detect the corresponding primary antibodies. Immune complexes were visualized using an enhanced chemiluminescence detection kit (ECL Plus, Amersham Pharmacia Biotech) and Versadoc 5000 Imaging System (Bio-Rad) following manufacturers' instructions, and quantified with Quantity One (Bio-Rad) software. Results of Western blot analyses shown in this report are representative of two to four independent experiments.

In vivo SUMOylation Assay

For *in vivo* SUMOylation analyses of HMGA2, COS-1 cells were transiently transfected with EGFP-SUMO-1 and HA-tagged HMGA2 expression constructs. After 36 h, cells were lysed directly in 200 μL of SDS lysis buffer as described above. Lysates were further boiled for 5 min and equal amounts of proteins were fractionated by SDS-PAGE, followed by Western blot analyses with an anti-HA and/or an anti–SUMO-1 antibody (anti-GMP, Zymed Laboratories).

In vitro SUMOylation Assay

The *in vitro* SUMOylation assays were done as described by Tatham et al. (22). Briefly, a combination of E1 enzyme (4 μg), E2 Ubc9 enzyme (2 μg), SUMO-1 (2 μg), and His-tagged HMGA2 (5 μg) were mixed with His-RanBP2 (2629–2710) or glutathione *S*-transferase PIAS1, in 20 μL SUMOylation buffer. The SUMOylation reaction was incubated at 30°C for 3 h. SDS lysis buffer was used to terminate the reaction and 5% of the reaction product was subjected to Western blot analyses.

Fluorescence and Immunofluorescence Microscopy Analyses

After transient transfection, Pa-4 and Pa-4/HMGA2 cells cultured on glass coverslips were fixed with 4% paraformaldehyde in 1× PBS for 30 min at room temperature. The cells were quenched with 50 mmol/L ammonium chloride in PBS for 5 min and blocked with 1% bovine serum albumin in PBS before mounting with Antifade Reagent (Molecular Probes). Cells were examined using a Nikon PCM 2000 confocal system (Center for Liver Diseases, University of Southern California). For the confocal analyses, serial images were obtained with a Nikon PCI System confocal microscope and processed by Metamorph Imaging Software for three-dimensional and orthogonal plane reconstruction. To estimate the effect of HMGA2 on the average number of PML nuclear body and average volume of PML nuclear body, Pa-4 cells were transiently transfected with 0.1 μg PML-expressing construct in the presence or absence of HMGA2. Twenty-four hours after transfection, cells were processed for immunocytochemistry following the procedure described above for volume measurement and Integrated Morphometric Analysis.

For immunofluorescence microscopy analyses, transiently transfected Pa-4 and Pa-4/HMGA2 cells cultured on glass coverslips were fixed and quenched as above, followed by washing with PBS, permeabilization with 0.5% Triton X-100 in PBS for 15 min, PBS washing again, and finally blocking with 1% bovine serum albumin in PBS. Cells were first incubated with the appropriate primary antibody, washed with PBS, and then exposed to the appropriate secondary conjugates including goat–anti-rabbit IgG rhodamine conjugate (Santa Cruz Biotechnology), goat–anti-mouse IgG FITC conjugate (Santa Cruz Biotechnology), goat–anti-mouse IgG Alexa Fluor 350 (Molecular Probes), respectively, and 4′,6-diamidino-2-phenylindole, followed by PBS wash. Finally, the signals from cells were examined using Metamorph Imaging System in a Nikon microscope (Center for Liver Diseases, University of Southern California). All images were processed with Adobe Photoshop 7.0 software and then phenotypically classified and quantified.

Results

HMGA2 Is SUMOylated *In vitro* and *In vivo*

Previous studies by us and other groups have shown that aberrant expression of architectural transcription factor HMGA2 is associated with the regulation of cell proliferation and gene expression (8,19,20,23,24). We therefore sought to screen for novel HMGA2-interacting proteins that mediate the pleiotropic effects by HMGA2. By using LexA-HMGA2 as the bait in yeast two-hybrid screens, we have identified E2 SUMO-conjugating enzyme Ubc9 and SUMO-1 as HMGA2-interacting proteins (Supplementary Fig. S1).[5] Because many SUMOylation targets were identified as SUMO-1– and Ubc9-interacting proteins, we did *in vitro* SUMOylation assays by using His-tagged HMGA2 as the substrate to test whether HMGA2 can be SUMO-1 modified. Recombinant HMGA2 protein was prepared and subjected to *in vitro* SUMOylation assays in the presence of a combination of SUMO-activating enzyme

[5]Supplementary material for this article is available at Molecular Cancer Therapeutics Online (http://mct.aacrjournals.org/).

(Aos1-Uba2), Ubc9 and SUMO-1. As shown in Fig. 1A, a slower migrating form of HMGA2 was exclusively observed in the presence of E1/E2/SUMO-1 (*lanes 1*, *5*, and *6* versus *lanes 2 –4*), indicating that HMGA2 was covalently modified by SUMO-1. It was apparent that both RanBP2 (2629–2710) and PIAS1 could serve the function of E3-ligase to stimulate SUMO-1 conjugation to HMGA2 *in vitro* (Fig. 1A, *lanes 5* and *6* versus *lane 1*).

Next, we examined whether HMGA2 could be SUMOylated *in vivo*. To this end, we coexpressed HA-tagged HMGA2 and EGFP-tagged SUMO-1 in COS-1 cells and did Western analyses of whole-cell lysates using an anti-HA antibody. The anti-HA antibody detected SUMO-modified HMGA2 in addition to the original HA-tagged HMGA2 (Fig. 1B and C). To ensure that this SUMO-1–dependent HA-immunoreactive species was indeed the SUMO-1–modified HMGA2, we coexpressed HA-HMGA2 and EGFP-SUMO-1aa, in which the COOH-terminal Gly-Gly amino acid residues required for SUMOylation were mutated to Ala-Ala, in COS-1 cells. Upon the coexpression with EGFP-SUMO-1aa, the higher molecular mass HMGA2 species observed with EGFP-SUMO-1 was not detected (Fig. 1B, *lane 5* versus *lane 4*). Moreover, the signal of this SUMO-1–modified species intensified in a dose-dependent manner with increasing amounts of EGFP-SUMO-1 (Fig. 1C, *top, lanes 4* and *5*). ΔAxam was identified as a deSUMOylase for a variety of SUMOylated proteins (25, 26). To further ascertain that HMGA2 is a SUMOylation target, COS-1 cells were transfected with a combination of expression constructs harboring HMGA2, EGFP-SUMO-1, and ΔAxam. As shown in Fig. 1C, a reduced level of SUMOylated HMGA2 was observed with increasing amounts of cotransfected ΔAxam (*bottom, lanes 5* and *6* versus *lane 4*). Taken together, these findings clearly showed that HMGA2 is indeed a substrate of SUMOylation.

Although HMGA2 has been shown herein to be SUMOylated *in vitro* and *in vivo* (Fig. 1A and B), it does not harbor the canonical SUMOylation target sequence, namely ψKXE (where ψ is a large hydrophobic amino acid, most commonly Ile or Val, and X is any residue; refs. 10–12). The Lys residues at positions 66 and 67 of HMGA2 bear homology with ψKXE (Fig. 1D, *top*). To determine whether these two Lys residues are involved in HMGA2 SUMOylation, we mutated these Lys residues to Arg and analyzed its effect on HMGA2 SUMOylation. A HMGA2(4P/A) mutant containing four Pro to Ala mutations at amino acid positions 48, 52, 76, and 80, which are located within the second and third DNA-binding AT-hook domains of HMGA2 (Fig. 1D, *top*) and are reported to abolish its DNA binding ability (27), was also engineered to serve as a negative control for our SUMOylation assays. As shown in Fig. 1D, cells transfected with HMGA2 harboring 4P/A mutations displayed a SUMOylation pattern similar to the wild-type HMGA2 (*bottom, lane 6* versus *lane 3*), whereas 2K/R mutations almost completely prevented the formation of SUMO-1–modified HMGA2 (*bottom, lane 5* versus *lane 3*), suggesting that HMGA2(2K/R) is SUMOylation defective.

HMGA2, but not SUMOylation-Defective HMGA2 (2K/R), Down-Regulates PML

While analyzing images from confocal microscopy to investigate whether SUMOylation affects HMGA2 cellular localization, we noticed that both the average number and the size of PML nuclear body per cell decreased unexpectedly in Pa-4/HMGA2 cells (Fig. 2A, *a* and *b*). By performing three-dimensional reconstructions from serial confocal cross-sections of PML nuclear bodies, we quantified these changes associated with PML between Pa-4 and Pa-4/HMGA2 cells. As shown in Fig. 2A, the average number of PML nuclear body per Pa-4/HMGA2 cell decreased by 30% compared with that in individual Pa-4 cell (*c*). Furthermore, HMGA2 also reduced the relative amount of PML protein assembled into each PML nuclear body by ~25% (*d*), as determined by measuring the average volume of nuclear space occupied by PML inside each PML nuclear body. We next examined whether HMGA2 causes a reduction in the steady-state levels of PML by Western analyses. As shown in Fig. 2B, a marked decrease in the intensity of both PML and SUMO-1–modified PML by HMGA2 was observed

(*top, lanes 5* and *6* versus *lane 4*), resulting from the combined effects by HMGA2 on both the average number of PML nuclear body per cell and the relative amount of PML per PML nuclear body. By contrast, the effect of SUMOylation-defective HMGA2(2K/R) on the steady-state levels of PML and SUMOylated PML was negligible (Fig. 2B, *top, lanes 7* and *8* versus *lane 4*). To address whether this HMGA2-mediated down-regulation is specific to PML, we assessed the steady-state level of glucocorticoid receptor (GR), another known SUMOylation target, to see if it is also reduced upon HMGA2 expression by Western analyses. As shown in Fig. 2B, HMGA2 did not reduce the steady-state level of either SUMOylated or unSUMOylated GR (*bottom, lane 4* versus *lane 2*). The well-established dexamethasone-mediated GR down-regulation (28) was used to validate our assays (Fig. 2B, *bottom, lane 3* versus *lane 2*).

To rule out that this HMGA2-dependent down-regulation is an artifact of PML overexpression, we next investigated the effect of HMGA2 on the steady-state levels of both endogenous forms of PML (unSUMOylated and SUMOylated) and endogenous SUMOylated RanGAP-1 using Pa-4 cells and their stable HMGA2-expressing Pa-4/HMGA2 cells. We found that HMGA2 affects the stability of both SUMOylated and unSUMOylated forms of endogenous PML, but not of endogenous SUMOylated RanGAP-1 (Fig. 2C). Consistent with Fig. 2B, SUMOylation-defective HMGA2(2K/R) also failed to decrease the steady-state level of both SUMOylated and unSUMOylated forms of endogenous PML (Fig. 2D). Taken together, we concluded that HMGA2 selectively decreases the steady-state level of PML, but not RanGAP-1 and GR (Fig. 2B and C), and that the observed effect by HMGA2 is, at least in part, dependent on its SUMOylation capacity (Fig. 2D).

Arsenic Trioxide Induces Transient HMGA2 SUMOylation and Association of HMGA2 Foci with PML Nuclear Body

It has been reported that PML SUMOylation is regulated by pharmacologic agents, such as arsenic trioxide (ATO; refs. 29–31). We then tested the possibility that HMGA2 SUMOylation could be regulated by ATO treatment and used ATO-induced PML SUMOylation as a control. As shown in Fig. 3A, the intensity of SUMOylated HMGA2 was enhanced by ATO (1 μmol/L) treatment (*lane 4* versus *lane 3*). However, we also noted that ATO failed to render a marked accumulation of SUMO-conjugated PML in Pa-4/HMGA2 cells (Fig. 3B, *lane 6* versus *lane 5*), whereas ATO stimulated PML SUMOylation in Pa-4 cells (Fig. 3B, *lane 3* versus *lane 2*) as reported in the literature (29–31), further supporting the notion that HMGA2 selectively decrease PML protein levels.

SUMOylation is often involved in regulating protein function through protein-protein interaction, subcellular compartmentalization, and association with PML nuclear bodies (13, 14,29–31). To understand the possible mechanism underlying HMGA2-mediated PML down-regulation, we next investigated whether SUMOylation affects the relative nuclear compartmentalization of HMGA2 and PML by confocal microscopy analyses. Consistent with previous reports (13,14), treatment of ATO (1 μmol/L) for 1 hour reproducibly led to the maturation of PML nuclear bodies (Fig. 3C, *e* versus *b*). Intriguingly, upon the exposure of ATO, HMGA2 accumulated as visible hollow bodies within the nucleus (Fig. 3C, *d*), which were not clearly visible before ATO exposure (Fig. 3C, *a*). In addition, HMGA2 surrounded the periphery of the PML nuclear body in ATO-treated cells (Fig. 3C, *f* versus *c*) in almost all the cells we examined (data not shown). The ATO-induced partial colocalization of HMGA2 and PML was further confirmed by reconstructing the horizontal and vertical cross-sections of the HMGA2 foci and PML nuclear body (Fig. 3C, *h*). By contrast, eliminating SUMOylation capacity of HMGA2 and PML, that is, HMGA2(2K/R) and PMLΔS, almost completely abolished the ATO-induced HMGA2 foci formation (Fig. 3D, *d*) and HMGA2 partial colocalization with PML (Fig. 3D, *f* and *h*).

The HMGA2-Mediated PML Destabilization Is SUMOylation Dependent

To further explore the contribution of PML SUMOylation to HMGA2-dependent PML degradation, we measured the steady-state level of PML and SUMOylation-defective PML, PMLΔS, in the presence of HMGA2. We found that the steady-state level of PML, but not PMLΔS, was markedly reduced by HMGA2 in a dose-dependent manner (Fig. 4A, *top left* versus *bottom left*). We next examined the effect of ectopic expression of SUMO-1 with or without ATO treatment on the modulation HMGA2-mediated PML degradation. Consistent with Fig. 2B, combined action by SUMO-1 and ATO stimulated the degradation of PML in Pa-4/HMGA2 (Fig. 4A, *bottom right, lanes 2* and *3* versus *lane 1*), but not Pa-4, cells (Fig. 4A, *top right, lanes 2* and *3* versus *lane 1*). By contrast, the combination of SUMO-1 and ATO failed to induce PMLΔS down-regulation in Pa-4/HMGA2 cells (Fig. 4A, *bottom right, lanes 5* and *6* versus *lane 4*). These findings indicated that K/R mutations in PMLΔS render it relatively resistant to HMGA2-elicited destabilization of PML. To ascertain the contribution of SUMO-1 to HMGA2-elicited PML degradation, we covalently attached SUMO-1 in-frame to HMGA2 and HMGA2(2K/R) to engineer SUMO-HMGA2 and SUMO-HMGA2(2K/R), respectively (Fig. 4B, *top*). A similar approach was used to show the transcriptional repression property of SUMO in SUMOylated Sp3 (32). As expected, both SUMOylation-mimetic SUMO-HMGA2 and SUMO-HMGA2(2K/R) were more potent than their respective counterparts, remarkably enhancing the degradation of steady-state level of PML (Fig. 4B, *bottom, lane 3* versus *lane 2* and *lane 6* versus *lane 5*), whereas SUMOylation-defective HMGA2(2K/R) failed to promote PML degradation (Fig. 4B, *bottom, lane 5* versus *lanes 4* and *6*). Because all four HMGA2 expression constructs expressed comparably (Fig. 4B, *second* and *third panels*), we conclude that SUMOylation of HMGA2 may decrease PML stability or synthesis.

Lastly, we wanted to confirm that there is a possible biological consequence that results from HMGA2-promoted PML down-regulation. We have previously shown that PML SUMOylation plays a major role in stimulating GR transactivation (13); we hence predicted that HMGA2 would repress GR transactivation potential by decreasing endogenous PML/SUMOylated PML level. As expected, HMGA2 inhibited GR/dexamethasone–activated $(TAT)_3$-Luc activity (Fig. 4C, *lane 5* versus *lane 2*), and PML, but not PMLΔS, alleviated the repressive effect by HMGA2 in a dose-dependent manner (Fig. 4C, *lanes 6 –8* versus *lanes 9 –11*). To confirm this observation, Pa-4 cells were transiently cotransfected with pG5-Luc reporter and pGal4-GRAF1 in the presence or absence of PML or PMLΔS and HMGA2 or its mutants. As depicted in Fig. 4D, PML, but not PMLΔS, enhanced pGal4-GRAF1 transactivation (*lanes 2* and *6* versus *lane 1*). Moreover, HMGA2(4P/A) mutant, albeit to a lesser extent, diminished the enhancing effect of PML on pGal4-GRAF1 as HMGA2 wild-type did (Fig. 4D, *lanes 3* and *4* versus *lane 2*). Importantly, SUMOylation-defective HMGA2 (2K/R) mutant failed to repress PML-stimulated GRAF1 activation (Fig. 4D, *lane 5* versus *lane 2*). Taken together, our studies indicated that the functional antagonism between HMGA2 and PML is SUMOylation dependent.

Ubiquitin-Proteasome – Dependent Degradation Is Involved in HMGA2-Mediated Down-Regulation of PML

Short-term ATO treatment reportedly increases PML level (30), which could be used as a means to further exemplify the effect by HMGA2 on the PML protein level and to investigate the underlying mechanism. We then measured the steady-state level of PML in Pa-4 and Pa-4/HMGA2 cells upon the exposure of ATO and confirmed that ATO treatment (1 hour) induces the up-regulation of PML in a concentration-dependent manner in Pa-4 cells (Fig. 5A, *top left, lanes 3* and *4* versus *lane 2*). By contrast, there was no PML up-regulation observed in ATO-treated Pa-4/HMGA2 cells (Fig. 5A, *bottom left, lanes 3* and *4* versus *lane 2*). Because HMGA2 decreased both endogenous and ectopically expressed PML protein levels (Figs. 2B and D,

and 5A), we postulated that HMGA2 could promote PML protein degradation. To examine this possibility, we assessed whether ubiquitin-proteasome–dependent protein degradation participates in HMGA2-mediated down-regulation of the steady-state level of PML. Because proteins degraded by the proteasome pathway are usually tagged with polyubiquitin (33), we then examined the contribution of ubiquitin to HMGA2-mediated reduction of PML level. To achieve this goal, Pa-4 cells were cotransfected with PML and a combination of ubiquitin and HMGA2. As shown in Fig. 5A (*right*), HMGA2 caused a concordant decrease of ubiquitin-PML and PML (*lane 3* versus *lane 2*). It also seemed that ectopic expression of ubiquitin further enhanced the effect of HMGA2 in decreasing the steady-state level of PML protein (Fig. 5A, *right, lane 3* versus *lane 4*).

We also wished to investigate whether HMGA2-dependent PML down-regulation can be extended to other cell types. To this end, we established stably transfected HeLa/HMGA2 cells and adapted an ATO treatment paradigm to investigate the effect of HMGA2 on PML degradation. Consistent with Fig. 5A, a decrease in PML protein level was noticed in ATO-treated HeLa/HMGA2 cells (Fig. 5B, *lane 6* versus *lane 5*), whereas PML accumulated in HeLa cells that were subjected to a comparable ATO treatment (Fig. 5B, *lane 3* versus *lane 2*). Furthermore, cotreatment of a selective proteasome inhibitor, epoxomicin (0.1 μmol/L), reversed, at least in part, the decrease of PML protein level in HeLa/HMGA2 cells (Fig. 5B, *lane 7* versus *lane 6*). A similar inhibitory effect by proteasome inhibitor, MG132, on HMGA2-dependent down-regulation of PML was also observed in Pa-4 cells (Fig. 5C, *lanes 2* and *3* versus *lane 1*). Importantly, there was noticeable accumulation of ubiquitin-PML detected in HMGA2-expressing Pa-4 cells (Fig. 5C, *lane 1* versus *lane 4*), which was further increased upon MG132 treatment (Fig. 5C, *lanes 2* and *3* versus *lane 1*), further supporting the involvement of the ubiquitin and proteasome in this HMGA2-dependent event. Some of these multiple PML species observed here and in other figures may represent differentially phosphorylated PML, as shown by Hayakawa and Privalsky (29). However, the exact role by phosphorylation to modulate HMGA2-promoted PML degradation remains to be investigated. Lastly, we transfected HeLa/HMGA2 cells with siRNA against ubiquitin (si-Ub) to knock down endogenous ubiquitin or with scrambled siRNA as a control (data not shown). As shown in Fig. 5D, transfection of si-Ub resulted in an accumulation of PML (*lane 3* versus *lane 2*), whereas scrambled siRNA elicited no visible effect (*lane 4* versus *lane 2*) in ATO-treated HeLa/HMGA2 cells. Together, we conclude that HMGA2 down-regulates PML protein level partly through ubiquitin-proteasome–dependent protein degradation. Our discovery revealed a previously undiscovered, SUMOylation-dependent function of HMGA2 in promoting PML degradation and broadened our understanding of mechanisms underlying the pleiotropic function of HMGA2.

Discussion

In this report, we provide evidence that HMGA2 can be modified by SUMO-1 and that this modification is responsible for HMGA2-promoted PML degradation. To our knowledge, HMGA2 is the first nonhistone chromosomal architectural protein reported to be SUMOylated. Posttranslational modifications of HMGA2 have been shown to have a profound effect on its biochemical and biological functions. For example, phosphorylation of the Ser residues located at the COOH terminus could affect HMGA2 DNA binding affinity (1,34,35) and phosphorylation of HMGA2 by Nek2 is essential for chromatin condensation in meiosis (36). Despite these extensive studies on HMGA2, the regulation of HMGA2 function by SUMOylation has remained largely unnoticed. We provide evidence herein that SUMOylation of HMGA2 plays a critical role in stimulating HMGA2 function in decreasing PML protein level via an ubiquitin-proteasome–dependent protein degradation. It is noteworthy that HMGA2-mediated promotion of protein degradation is exclusive for PML or SUMOylated PML, and is not extended to GR, SUMOylated GR, and RanGAP-1 (Fig. 2).

To our knowledge, this report represents the first demonstration that HMGA2 promotes PML degradation. Results from a number of *in vitro* and transgenic models and human cancer studies have established a direct correlation between a high expression level of HMGA family members and increasing degrees of neoplastic transformation (3,7,9). For example, HMGA2 interacts with pRB to displace HDAC1, resulting in the enhanced activity of E2F1 (37). Our results herein propose an additional pathway, namely HMGA2-promoted PML protein degradation, underlying the oncogenic ability of HMGA2. Based on published literature, PML protein is the only known target, thus far, for HMGA2-promoted protein degradation through the ubiquitin-proteasome–dependent pathway. Although PML protein has been reportedly degraded via proteasome by herpes virus and SIAHs (mammalian homologues of *Drosophila* Seven in Absentia; refs. 38,39), the enzymes that catalyze PML ubiquitination are still unspecified. Very recently, Scaglioni et al. (40) reported that casein kinase 2 phosphorylates Ser-517 of PML, rendering an enhanced ubiquitin-mediated degradation of PML. However, Ser-517 equivalency could not be located in the human PML-1 cDNA that was used in our studies reported here (41). These observations that HMGA2 down-regulates both ectopic and endogenous PML expressions further support the notion that HMGA2 uses a casein kinase 2–independent mechanism to promote PML degradation via proteasome. To prove the principle that HMGA2-promoted PML degradation is biologically relevant, we showed that this process can be stimulated by ATO treatment and that HMGA2 counteracts PML-mediated enhancement of GR transactivation. Besides stimulating GR function (13,42), PML nuclear bodies are reportedly involved in the cellular response to DNA damage (43). For example, components of the DNA damage sensor MRN complex are also reported to be colocalized with PML or PML nuclear bodies (43–47). Therefore, the aberrant expression HMGA2 is of pathologic and/or prognostic importance for a variety of neoplasia given that the modulation of the steady-state level of PML protein or PML nuclear body by HMGA2 affects many aspects of cellular processes.

Mechanistically, we have shown that the SUMOylation capacities of both HMGA2 and PML are required for the recruitment of HMGA2 around PML nuclear body (Fig. 3) and HMGA2-promoted PML degradation (Fig. 4) in ATO-treated cells. SUMOylation of PML has been proposed to play a major role in the recruitment of nuclear proteins, such as Sp100, Daxx, and PML itself, to the PML nuclear body and all these proteins have shown to be colocalized with PML within the PML nuclear body (13,48,49). By contrast, HMGA2 is recruited around, but not inside, the PML nuclear body upon ATO treatment (Fig. 3C). Although the molecular mechanism remains to be established, the accumulation of HMGA2 surrounding PML nuclear body could result in the subsequent PML degradation via ubiquitin-proteasome system. Alternatively, SUMOylated HMGA2 may compete with SUMO-modified PML for the same binding partners in the PML nuclear body and displace PML proteins. An advantage of such a combined covalent modification of HMGA2 by SUMO-1 and the recruitment of HMGA2 around PML nuclear body is the transient and rapid augmentation of its subsequent signaling in response to different milieu. In addition, the mutation of three Lys residues in PMLΔS could interfere with the process of proteasome recruitment to PML nuclear body (31), further supporting our proposed model. However, we were unable to coimmunoprecipitate HMGA2 and PML. One plausible explanation is that such an interaction is SUMO dependent, transient, and subsequently leads to PML degradation, which would make it challenging to recapitulate HMGA2/PML interaction by coimmunoprecipitation followed by Western analyses.

Recently, Narita et al. (50) reported that HMGA2 contributes to the malignant transformation of human diploid fibroblasts only when the senescence pathway is completely blocked. As PML is known as a tumor suppressor (17), our findings that HMGA2 promotes the degradation of PML may thus provide an additional molecular explanation for the (patho)physiologic function of HMGA2 and unequivocally show a previously unrecognized role of HMGA2 during tumorigenesis. It is also possible that the SUMO-dependent enhancement of HMGA2-

mediated event(s) is part of a larger mechanism that regulates HMGA2 function. Given the fact that the alterations in HMGA2 expression levels have been observed in a variety of human tumors and cancer cells (1), these presented results bring additional insights into HMGA2 biology as well as perhaps the role of HMGA2 in tumorigenesis. An even more comprehensive understanding of the molecular basis for HMGA2 function will extend our outlook for additional targets for cancer therapy.

Supplementary Material

Refer to Web version on PubMed Central for supplementary material.

Acknowledgments

Grant support: NIH research grants R01 DE 10742 and DE 14183 (D.K. Ann), and CA 94595 (Y. Chen); and Taiwan National Health Research Institutes grant MG-092-PP-03 (H.M. Shih). The imaging studies in this work were supported in part by NIH P30 DK48522 (Confocal Microscopy Subcore, University of Southern California Center for Liver Diseases).

We thank Allen Chang and Li-peng Yap for technical assistance, Dr. Michael R. Stallcup (University of Southern California) for critical reading and suggestions, Dr. Sarah Hamm-Alvarez (University of Southern California) for her suggestions and assistance on the image analyses, members of the Ann laboratory for helpful discussion and for sharing the reagents, and Eve Hu for editing the manuscript.

References

1. Sgarra R, Rustighi A, Tessari MA, et al. Nuclear phosphoproteins HMGA and their relationship with chromatin structure and cancer. FEBS Lett 2004;574:1–8. [PubMed: 15358530]
2. Wolffe AP. Architectural transcription factors. Science 1994;264:1100–1. [PubMed: 8178167]
3. Abe N, Watanabe T, Suzuki Y, et al. An increased high-mobility group A2 expression level is associated with malignant phenotype in pancreatic exocrine tissue. Br J Cancer 2003;89:2104–9. [PubMed: 14647145]
4. Finelli P, Pierantoni GM, Giardino D, et al. The high mobility group A2 gene is amplified and overexpressed in human prolactinomas. Cancer Res 2002;62:2398–405. [PubMed: 11956103]
5. Masciullo V, Baldassarre G, Pentimalli F, et al. HMGA1 protein overexpression is a frequent feature of epithelial ovarian carcinomas. Carcinogenesis 2003;24:1191–8. [PubMed: 12807722]
6. Berlingieri MT, Manfioletti G, Santoro M, et al. Inhibition of HMGI-C protein synthesis suppresses retrovirally induced neoplastic transformation of rat thyroid cells. Mol Cell Biol 1995;15:1545–53. [PubMed: 7862147]
7. Fedele M, Battista S, Kenyon L, et al. Overexpression of the HMGA2 gene in transgenic mice leads to the onset of pituitary adenomas. Oncogene 2002;21:3190–8. [PubMed: 12082634]
8. Miyazawa J, Mitoro A, Kawashiri S, Chada KK, Imai K. Expression of mesenchyme-specific gene HMGA2 in squamous cell carcinomas of the oral cavity. Cancer Res 2004;64:2024–9. [PubMed: 15026339]
9. Langelotz C, Schmid P, Jakob C, et al. Expression of high-mobility-group-protein HMGI-C mRNA in the peripheral blood is an independent poor prognostic indicator for survival in metastatic breast cancer. Br J Cancer 2003;88:1406–10. [PubMed: 12778070]
10. Bossis G, Melchior F. SUMO: regulating the regulator. Cell Division 2006;1:13. [PubMed: 16805918]
11. Gill G. SUMO and ubiquitin in the nucleus: different functions, similar mechanisms? Genes Dev 2004;18:2046–59. [PubMed: 15342487]
12. Hay RT. SUMO: a history of modification. Mol Cell 2005;18:1–12. [PubMed: 15808504]
13. Lin DY, Lai MZ, Ann DK, Shih HM. Promyelocytic leukemia protein (PML) functions as a glucocorticoid receptor co-activator by sequestering Daxx to the PML oncogenic domains (PODs) to enhance its transactivation potential. J Biol Chem 2003;278:15958–65. [PubMed: 12595526]

14. Sachdev S, Bruhn L, Sieber H, Pichler A, Melchior F, Grosschedl R. PIASy, a nuclear matrix-associated SUMO E3 ligase, represses LEF1 activity by sequestration into nuclear bodies. Genes Dev 2001;15:3088–103. [PubMed: 11731474]
15. Ishov AM, Sotnikov AG, Negorev D, et al. PML is critical for ND10 formation and recruits the PML-interacting protein daxx to this nuclear structure when modified by SUMO-1. J Cell Biol 1999;147:221–34. [PubMed: 10525530]
16. Borden KL. Pondering the promyelocytic leukemia protein (PML) puzzle: possible functions for PML nuclear bodies. Mol Cell Biol 2002;22:5259–69. [PubMed: 12101223]
17. Salomoni P, Pandolfi PP. The role of PML in tumor suppression. Cell 2002;108:165–70. [PubMed: 11832207]
18. Takahashi Y, Lallemand-Breitenbach V, Zhu J, de The H. PML nuclear bodies and apoptosis. Oncogene 2004;23:2819–24. [PubMed: 15077145]
19. Li D, Lin HH, McMahon M, Ma H, Ann DK. Oncogenic raf-1 induces the expression of non-histone chromosomal architectural protein HMGI-C via a p44/p42 mitogen-activated protein kinase-dependent pathway in salivary epithelial cells. J Biol Chem 1997;272:25062–70. [PubMed: 9312114]
20. Zentner MD, Lin HH, Deng HT, Kim KJ, Shih HM, Ann DK. Requirement for high mobility group protein HMGI-C interaction with STAT3 inhibitor PIAS3 in repression of α-subunit of epithelial Na^+ channel (α-ENaC) transcription by Ras activation in salivary epithelial cells. J Biol Chem 2001;276:29805–14. [PubMed: 11390395]
21. Kadoya T, Kishida S, Fukui A, et al. Inhibition of Wnt signaling pathway by a novel axin-binding protein. J Biol Chem 2000;275:37030–7. [PubMed: 10944533]
22. Tatham MH, Kim S, Jaffray E, Song J, Chen Y, Hay RT. Unique binding interactions among Ubc9, SUMO and RanBP2 reveal a mechanism for SUMO paralog selection. Nat Struct Mol Biol 2005;12:67–74. [PubMed: 15608651]
23. Boo LM, Lin HH, Chung V, et al. High mobility group A2 potentiates genotoxic stress in part through the modulation of basal and DNA damage-dependent phosphatidylinositol 3-kinase-related protein kinase activation. Cancer Res 2005;65:6622–30. [PubMed: 16061642]
24. Tessari MA, Gostissa M, Altamura S, et al. Transcriptional activation of the cyclin A gene by the architectural transcription factor HMGA2. Mol Cell Biol 2003;23:9104–16. [PubMed: 14645522]
25. Best JL, Ganiatsas S, Agarwal S, et al. SUMO-1 protease-1 regulates gene transcription through PML. Mol Cell 2002;10:843–55. [PubMed: 12419228]
26. Nishida T, Kaneko F, Kitagawa M, Yasuda H. Characterization of a novel mammalian SUMO-1/Smt3-specific isopeptidase, a homologue of rat axam, which is an axin-binding protein promoting β-catenin degradation. J Biol Chem 2001;276:39060–6. [PubMed: 11489887]
27. Himes SR, Reeves R, Attema J, Nissen M, Li Y, Shannon MF. The role of high-mobility group I(Y) proteins in expression of IL-2 and T cell proliferation. J Immunol 2000;164:3157–68. [PubMed: 10706706]
28. Deroo BJ, Rentsch C, Sampath S, Young J, DeFranco DB, Archer TK. Proteasomal inhibition enhances glucocorticoid receptor transactivation and alters its subnuclear trafficking. Mol Cell Biol 2002;22:4113–23. [PubMed: 12024025]
29. Hayakawa F, Privalsky ML. Phosphorylation of PML by mitogen-activated protein kinases plays a key role in arsenic trioxide-mediated apoptosis. Cancer Cell 2004;5:389–401. [PubMed: 15093545]
30. Kawai T, Akira S, Reed JC. ZIP kinase triggers apoptosis from nuclear PML oncogenic domains. Mol Cell Biol 2003;23:6174–86. [PubMed: 12917339]
31. Lallemand-Breitenbach V, Zhu J, Puvion F, et al. Role of promyelocytic leukemia (PML) sumolation in nuclear body formation, 11S proteasome recruitment, and As_2O_3-induced PML or PML/retinoic acid receptor α degradation. J Exp Med 2001;193:1361–71. [PubMed: 11413191]
32. Ross S, Best JL, Zon LI, Gill G. SUMO-1 modification represses Sp3 transcriptional activation and modulates its subnuclear localization. Mol Cell 2002;10:831–42. [PubMed: 12419227]
33. Ciechanover A. The ubiquitin-proteasome pathway: on protein death and cell life. EMBO J 1998;17:7151–60. [PubMed: 9857172]
34. Brants JR, Ayoubi TA, Chada K, Marchal K, Van de Ven WJ, Petit MM. Differential regulation of the insulin-like growth factor II mRNA-binding protein genes by architectural transcription factor HMGA2. FEBS Lett 2004;569:277–83. [PubMed: 15225648]

35. Noro B, Licheri B, Sgarra R, et al. Molecular dissection of the architectural transcription factor HMGA2. Biochemistry 2003;42:4569–77. [PubMed: 12693954]
36. Di Agostino S, Fedele M, Chieffi P, et al. Phosphorylation of high-mobility group protein A2 by Nek2 kinase during the first meiotic division in mouse spermatocytes. Mol Biol Cell 2004;15:1224–32. [PubMed: 14668482]
37. Fedele M, Visone R, De Martino I, et al. HMGA2 induces pituitary tumorigenesis by enhancing E2F1 activity. Cancer Cell 2006;9:459–71. [PubMed: 16766265]
38. Chelbi-Alix MK, de The H. Herpes virus induced proteasome-dependent degradation of the nuclear bodies-associated PML and Sp100 proteins. Oncogene 1999;18:935–41. [PubMed: 10023669]
39. Fanelli M, Fantozzi A, De Luca P, et al. The coiled-coil domain is the structural determinant for mammalian homologues of *Drosophila* Sina-mediated degradation of promyelocytic leukemia protein and other tripartite motif proteins by the proteasome. J Biol Chem 2004;279:5374–9. [PubMed: 14645235]
40. Scaglioni PP, Yung TM, Cai LF, et al. A CK2-dependent mechanism for degradation of the PML tumor suppressor. Cell 2006;126:269–83. [PubMed: 16873060]
41. Kakizuka A, Miller WH Jr, Umesono K, et al. Chromosomal translocation t(15;17) in human acute promyelocytic leukemia fuses RAR α with a novel putative transcription factor, PML. Cell 1991;66:663–74. [PubMed: 1652368]
42. Doucas V, Tini M, Egan DA, Evans RM. Modulation of CREB binding protein function by the promyelocytic (PML) oncoprotein suggests a role for nuclear bodies in hormone signaling. Proc Natl Acad Sci U S A 1999;96:2627–32. [PubMed: 10077561]
43. Evans JD, Hearing P. Relocalization of the Mre11-50-Nbs1 complex by the adenovirus E4 ORF3 protein is required for viral replication. J Virol 2005;79:6207–15. [PubMed: 15858005]
44. Carbone R, Pearson M, Minucci S, Pelicci PG. PML NBs associate with the hMre11 complex and p53 at sites of irradiation induced DNA damage. Oncogene 2002;21:1633–40. [PubMed: 11896594]
45. Iijima K, Komatsu K, Matsuura S, Tauchi H. The Nijmegen breakage syndrome gene and its role in genome stability. Chromosoma 2004;113:53–61. [PubMed: 15258809]
46. Jiang WQ, Zhong ZH, Henson JD, Neumann AA, Chang AC, Reddel RR. Suppression of alternative lengthening of telomeres by Sp100-mediated sequestration of the MRE11/RAD50/NBS1 complex. Mol Cell Biol 2005;25:2708–21. [PubMed: 15767676]
47. Xu ZX, Timanova-Atanasova A, Zhao RX, Chang KS. PML colocalizes with and stabilizes the DNA damage response protein TopBP1. Mol Cell Biol 2003;23:4247–56. [PubMed: 12773567]
48. Muller S, Matunis MJ, Dejean A. Conjugation with the ubiquitin-related modifier SUMO-1 regulates the partitioning of PML within the nucleus. EMBO J 1998;17:61–70. [PubMed: 9427741]
49. Zhong S, Muller S, Ronchetti S, Freemont PS, Dejean A, Pandolfi PP. Role of SUMO-1-modified PML in nuclear body formation. Blood 2000;95:2748–52. [PubMed: 10779416]
50. Narita M, Narita M, Krizhanovsky V, et al. A novel role for high-mobility group a proteins in cellular senescence and heterochromatin formation. Cell 2006;126:503–14. [PubMed: 16901784]

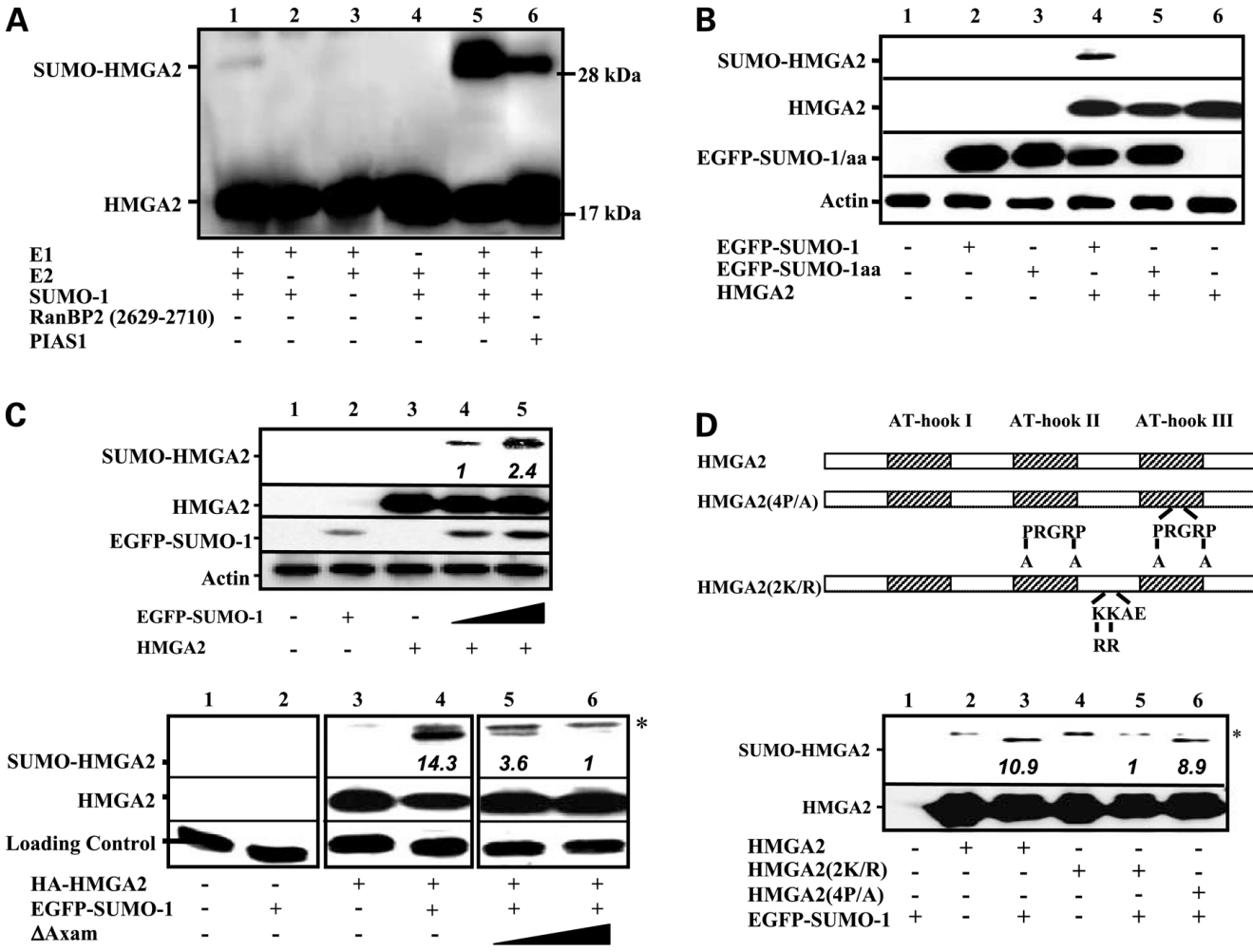

Figure 1.

HMGA2 is a SUMOylation target. **A,** HMGA2 is SUMOylated *in vitro. In vitro* SUMOylation reaction was done as described in Materials and Methods, and analyzed with the indicated antibodies. **B,** HMGA2 is modified by EGFP-SUMO-1, but not by EGFP-SUMO-1aa, *in vivo*. COS-1 cells were transfected with HMGA2, and EGFP-SUMO-1/EGFP-SUMO-1aa, as indicated. Cells were lysed and analyzed by immunoblotting using an anti-HA antibody to detect both HMGA2 and SUMOylated HMGA2. An anti-GFP antibody was used to detect EGFP-SUMO-1 and EGFP-SUMO-1aa. **C,** the effect of ΔAxam on HMGA2 SUMOylation. Whole-cell lysates of COS-1 cells expressing the indicated protein were probed with an anti-HA antibody. **D,** mapping the SUMO-1 modification site of HMGA2. The functional domains and mutation sites were schematically illustrated as in the top panel. *Hatched boxes,* the AT-hook DNA-binding domain. COS-1 cells were transfected with HMGA2, HMGA2(4P/A), and HMGA2(2K/R), respectively. * in **C** and **D**, nonspecific species while using a particular lot of an anti-HA antibody. Relative levels of SUMO-HMGA2 in **C** and **D**, after normalization, are indicated as italic.

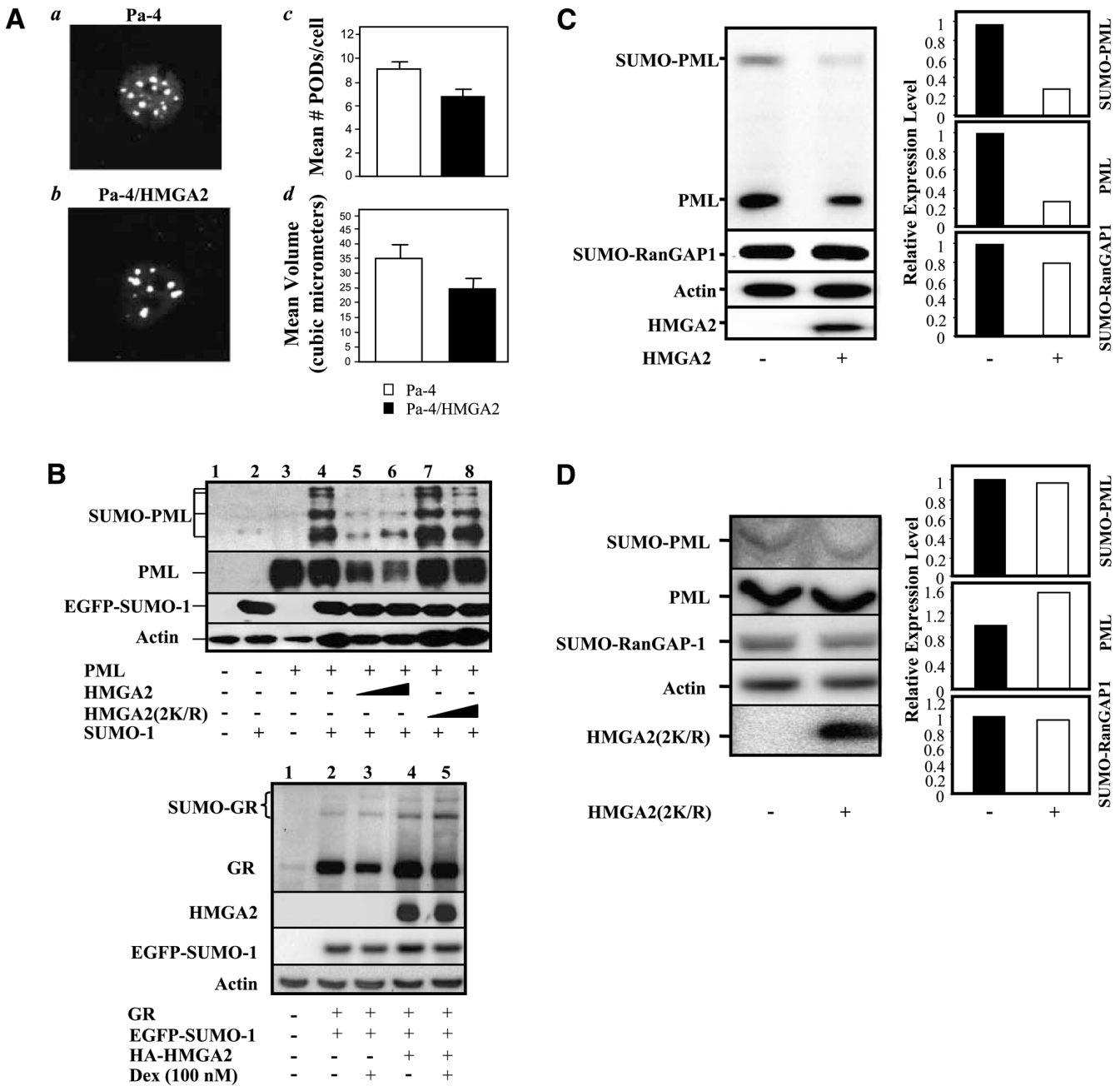

Figure 2.

HMGA2 down-regulates endogenous PML. **A,** HMGA2 reduces the size and number of PML nuclear body. Pa-4 (*a*) and Pa-4/HMGA2 (*b*) cells were transiently transfected with PML expression construct, respectively, and processed for immunocytochemistry analyses visualized with an anti-PML antibody as described in Materials and Methods. Morphometric parameters from *a* and *b* were measured by using Metamorph Imaging System and plotted to illustrate the decrease of average number of PML nuclear body per cell (*c*) and the reduction of PML volume assembled in each PML nuclear body (*d*). A total of 53 PML-transfected Pa-4 and 63 PML-transfected Pa-4/HMGA2 cells were examined in two quantitative analyses. *Columns*, mean based on two independent transfection experiments done in duplicates; *bars*, SD. **B,** HMGA2 selectively decreases the steady-state level of exogenous PML. COS-1 cells

were transiently transfected with PML, EGFP-SUMO-1, and increasing amounts of HA-HMGA2 and HA-HMGA2(2K/R), respectively. Total cell lysates was subjected to Western analyses with indicated antibodies (*top*). Pa-4 cells were transiently transfected with pKSX-GR and HMGA2 or vector in the presence of EGFP-SUMO-1 and treated with dexamethasone (*Dex*, 100 nmol/L) or vehicle as indicated, before protein extraction. Cell lysates was subjected to Western analyses with indicated antibodies (*bottom*). **C,** HMGA2 attenuates the steady-state level of endogenous PML without affecting SUMOylated RanGAP-1. Pa-4 cells were transfected with HMGA2 and cell lysates were subjected to Western analyses and probed for PML and SUMOylated PML (*top*) and SUMOylated RanGAP-1 (*middle panel 1*). Immunoreactive bands were quantitated by densitometry, and the relative intensity of the SUMOylated PML, PML, and SUMOylated RanGAP-1 was determined by normalizing with that of the corresponding actin signal. The relative expression level was then calculated by dividing the relative intensity (as determined above) of the HMGA2-transfected group by that of the corresponding group that was transfected with vector alone, which was arbitrarily designated as 1. **D,** SUMOylation of HMGA2 is required for HMGA2-mediated destabilization of endogenous PML and SUMOylated PML. Pa-4 cells were transfected with HMGA2(2K/R). Western analyses and data analyses were carried out as described in **C**.

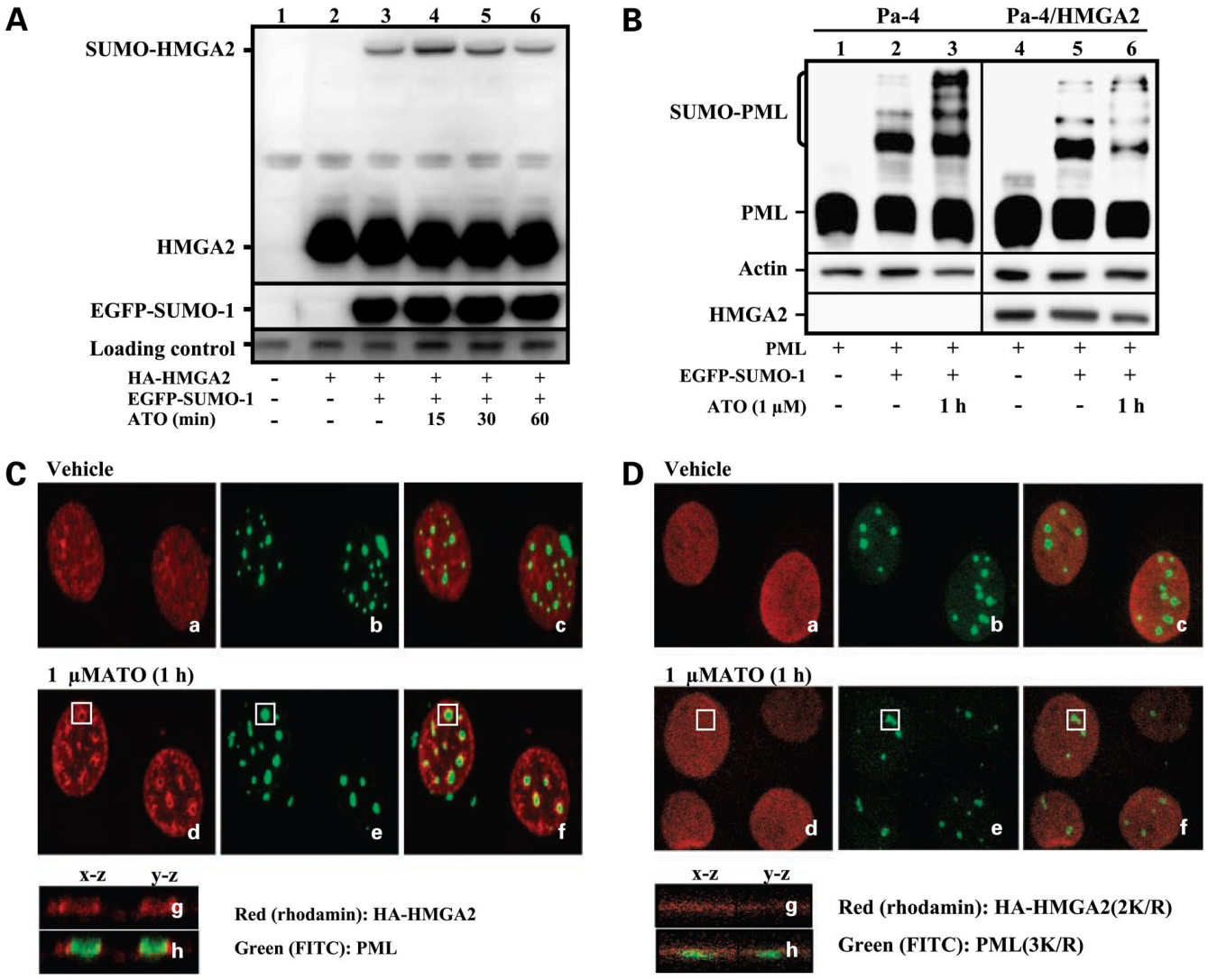

Figure 3.

ATO stimulates the partial colocalization between HMGA2 and PML. **A,** ATO transiently induces HMGA2 SUMOylation. COS-1 cells were transfected with HMGA2 and EGFP-SUMO-1, treated with 1 μmol/L ATO for the indicated time before protein extraction. Equal amounts of total lysates were subjected to Western analyses with an anti-HA antibody to detect HMGA2 and SUMOylated HMGA2. **B,** ATO renders differential accumulation of SUMOylated PML in Pa-4 and Pa-4/HMGA2 cells. Pa-4 and Pa-4/HMGA2 cells were transfected with a combination of PML and EGFP-SUMO-1 and followed with vehicle or ATO treatment for 1 h. Equal amounts of protein extracts were subjected to Western analyses with an anti-PML antibody to visualize PML and SUMO-conjugated PML. Actin was probed to ensure equal loading. **C,** HMGA2 surrounds PML nuclear body in ATO-treated cells. Pa-4/HMGA2 cells were transiently transfected with PML expression construct and treated with 1 μmol/L ATO for 1 h before confocal immunofluorescence analyses as described in Materials and Methods. The *x-z* section and *y-z* section of each indicated area in *d* and *f* were reconstructed in *g* and *h*, respectively. **D,** SUMOylation is required for ATO-induced PML and HMGA2 colocalization. Pa-4 cells were transiently cotransfected with SUMOylation-defective HMGA2(2K/R) and PMLΔS expression constructs and treated with 1 μmol/L ATO for 1 h before confocal immunofluorescence analyses as described in Materials and Methods. The *x-*

z section and *y*-*z* section of each indicated area in *d* and *f* were reconstructed in *g* and *h*, respectively.

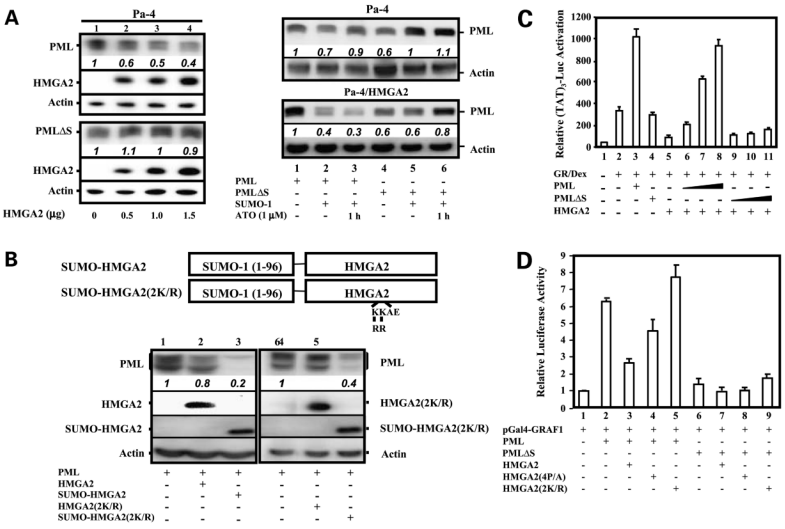

Figure 4.

SUMOylation is required for HMGA2 to destabilize PML. **A,** mutation on SUMOylation target of PML abolishes HMGA2-dependent PML degradation. Pa-4 cells were transiently transfected with PML (*top left*) or PMLΔS (*bottom left*) with an increasing amount of HMGA2. Cell extracts were collected and analyzed by immunoblotting with an anti-PML antibody. Anti-actin and anti-HA antibodies were used to probe the same membrane to ensure the equal loading and proper expression of HMGA2, respectively. Pa-4 and Pa-4/HMGA2 cells were transfected PML (*top right*) or PMLΔS (*bottom right*) with or without SUMO-1. The transfected cells were treated with vehicle or ATO (1 μmol/L) for 1 h before protein extraction. Relative levels of PML are indicated as italic. **B,** covalent attachment of SUMO-1 to HMGA2 accelerates HMGA2-mediated down-regulation of PML protein. SUMO-1 (1 –96) was engineered in-frame to HMGA2 or HMGA2(2K/R) to construct SUMO-HMGA2 and SUMO-HMGA2(2K/R), respectively (*top*). HeLa cells were transfected with a combination of PML, HMGA2, or its mutants, as indicated. Cells were harvested at 36 h posttransfection and whole-cell lysates were subjected to Western analyses. **C,** PML rescues the HMGA2-mediated transcriptional repression of GR. Pa-4 cells were transiently transfected with a combination of $(TAT)_3$-Luc, pRL-TK, GR, PML, PMLΔS, and HMGA2. After transfection, cells were cultured with a medium containing 0.05% fetal bovine serum before a treatment with either 100 nmol/L dexamethasone or vehicle. Both firefly and Renilla luciferase activities were measured simultaneously using the Dual-Luciferase Assay System (Promega). The level of induction by dexamethasone treatment, expressed as "relative $(TAT)_3$-Luc activation" is calculated by dividing the normalized reporter luciferase activity in extracts from dexamethasone-treated and transfected cells by that obtained from vehicle-treated and transfected cells. The normalized reporter activity from each vehicle-treated transfected cells was arbitrarily designated as 1. *Columns,* mean based on three independent transfection experiments done in duplicates; *bars,* SE. **D,** K/R mutations on HMGA2 abolish the repressing effect on PML-mediated GRAF1 activation. Pa-4 cells were transiently transfected with pRL-TK, pG5-Luc reporter gene, pGal4-GRAF1, and the combination of PML and HMGA2 as well as their mutants, as indicated. *Columns,* mean based on three independent transfection experiments done in duplicates; *bars,* SE.

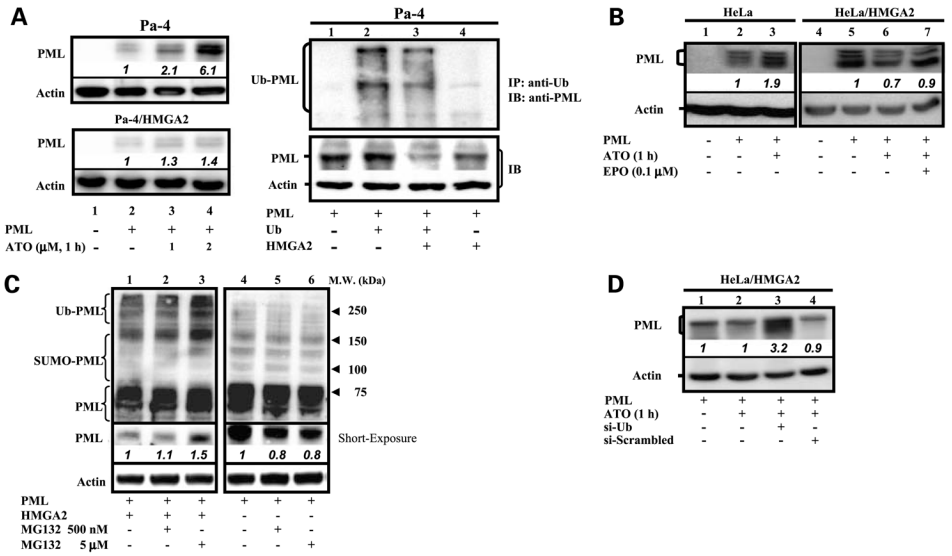

Figure 5.

The HMGA2-mediated PML destabilization is via proteasomes. **A,** HMGA2 enhances PML degradation. Pa-4 and Pa-4/HMGA2 cells were transiently transfected with PML or empty vector (*left*). Twenty-four hours after transfection, cells were treated with 0, 1, or 2 μmol/L ATO for 1 h before protein extraction. Pa-4 cells were transfected with PML and a combination of ubiquitin and HMGA2 (*right*). The whole-cell lysates were subjected to immunoprecipitation (*IP*) with an anti –c-myc antibody and followed by Western analyses (*IB*) using an anti-PML antibody. One tenth of the cellular lysates were also subjected to Western analyses to visualize the steady-state level of PML. An anti-actin antibody was also used to confirm equal loading. **B,** proteasome inhibitor blocks PML degradation in HeLa/HMGA2 cells. HeLa and HeLa/HMGA2 cells were transfected with PML expression construct. HeLa/HMGA2 cells were treated with epoxomicin (*EPO*; 0.1 μmol/L) for 16 h posttransfection (*lane 7*). Both HeLa and HeLa/HMGA2 cells were treated with 1 μmol/L ATO for 1 h before protein extraction. **C,** MG132 rescues PML from degradation in Pa-4/HMGA2, but not Pa-4 cells. Pa-4 and Pa-4/HMGA2 cells were transiently transfected with PML. Cells were treated with 0, 0.5, or 5 μmol/L MG132 (Calbiochem) for 2 h before protein extraction. The ubiquitin-PML (*Ub-PML*), SUMO-PML, and PML species were shown in the top. A short exposure of PML was also shown for the quantitation purpose (*second panel*). An anti-actin antibody was also used to confirm equal loading (*third panel*). The respective ubiquitin-PML and SUMO-PML species were further confirmed by using anti-ubiquitin and anti-SUMO antibodies, respectively (data not shown). **D,** si-Ub partially rescues PML in HeLa/HMGA2 cells. HeLa/HMGA2 cells transfected with PML and si-Ub or scrambled si-RNA and treated with 1 μmol/L ATO for 1 h before protein extraction. *Arrow*, accumulated PML species in si-Ub–, but not scrambled si-RNA–, transfected cells. Relative levels of PML in **A** (*left*), **B**, **C**, and **D** are indicated as italic.